

Phase separation in the vicinity of the surface of κ -(BEDT-TTF)₂Cu[N(CN)₂]Br by fast cooling

N. Yoneyama, T. Sasaki, and N. Kobayashi

Institute for Materials Research, Tohoku University, Sendai 980-8577, Japan

Y. Ikemoto and H. Kimura

Spring-8, Japan Synchrotron Radiation Research Institute, Mikazuki, Hyogo 679-5198, Japan

(Dated: November 17, 2018)

Partial suppression of superconductivity by fast cooling has been observed in the organic superconductor κ -(BEDT-TTF)₂Cu[N(CN)₂]Br by two means: a marked sample size effect on the magnetic susceptibility and direct imaging of insulating regions by scanning microregion infrared reflectance spectroscopy. Macroscopic insulating regions are proposed in the vicinity of the crystalline surface after fast cooling, with diameters of 50–100 μm and depths of a few μm . The very large in-plane penetration depth reported to date (~ 24 –100 μm) can be explained by the existence of the insulating regions.

I. INTRODUCTION

The magnetic penetration depth λ is one of the most fundamental parameters of superconductivity. It reflects the excitation of quasiparticles, governed by the superconducting (SC) gap symmetry. To clarify the mechanism of superconductivity, a careful study of the temperature dependence of λ is essential.

There have been many previous studies on the in-plane penetration depth λ_{\parallel} of the quasi-two-dimensional organic superconductors κ -(BEDT-

TTF)₂X [$X=\text{Cu}(\text{NCS})_2$ or $\text{Cu}[\text{N}(\text{CN})_2]\text{Br}$; BEDT-TTF: bis(ethylenedithio)-tetrathiafulvalene, also written as ET], by ac susceptibility,^{1,2,3,4} surface impedance,^{5,6} ac inductance⁷, μSR ,^{8,9,10,11} magnetization,^{12,13,14,15} etc. In spite of these efforts, the temperature dependence of λ_{\parallel} and the absolute value of $\lambda_{\parallel}(0)$ are still unknown or controversial. A precise determination of $\lambda_{\parallel}(0)$ is important for the superfluid density $\rho(T) = [\lambda_{\parallel}(T)/\lambda_{\parallel}(0)]^{-2}$; the behavior of $\rho(T)$ is strongly dependent on $\lambda_{\parallel}(0)$.⁷ However, the reported values of $\lambda_{\parallel}(0)$ for the two superconductors have large distributions, 0.4–2 μm [$X=\text{Cu}(\text{NCS})_2$] and 0.57–100 μm [$X=\text{Cu}[\text{N}(\text{CN})_2]\text{Br}$].¹⁵ We have recently found that these values of $\lambda_{\parallel}(0)$ can be classified into two groups:¹⁵ one for $\lambda_{\parallel}(0)$ larger than 1 μm and the other for shorter $\lambda_{\parallel}(0)$. The data in the first group were measured in magnetic fields lower than H_{c1} , in which a shielding current flows at the sample surface (shielding state). In this case, λ indicates the length from the surface H penetrates the sample. The data in the second group were measured in magnetic fields higher than H_{c1} , in which H penetrates into the sample as vortices (mixed state). In this case, λ is a decay length of the magnetic field from the center of a vortex.

A remarkable difference in $\lambda_{\parallel}(0)$ between the two groups appears for fast cooling, especially for $X = \text{Cu}[\text{N}(\text{CN})_2]\text{Br}$. In ac susceptibility measurements⁴ in magnetic fields lower than H_{c1} , $\lambda_{\parallel}(0)$ is 24–100 μm , which is two or three orders of magnitude larger than that obtained from magnetization measurements^{14,15} in magnetic fields higher than H_{c1} , $\sim 0.7 \mu\text{m}$. The former value of $\lambda_{\parallel}(0)$ is quite large as a characteristic parameter of superconductivity and is likely to be an overestimate. This measurement may be sensitive to the conditions of the first several layers of the surface, e.g., edge, step, and surface reconstruction.¹⁶ However, the fast cooling data of $\lambda_{\parallel}(0)$ in the low field measurements are still too large to be explained by these surface effects in the nanometer scale. This implies the existence of non-SC regions in the vicinity of the surface, probably in the macroscopic scale.

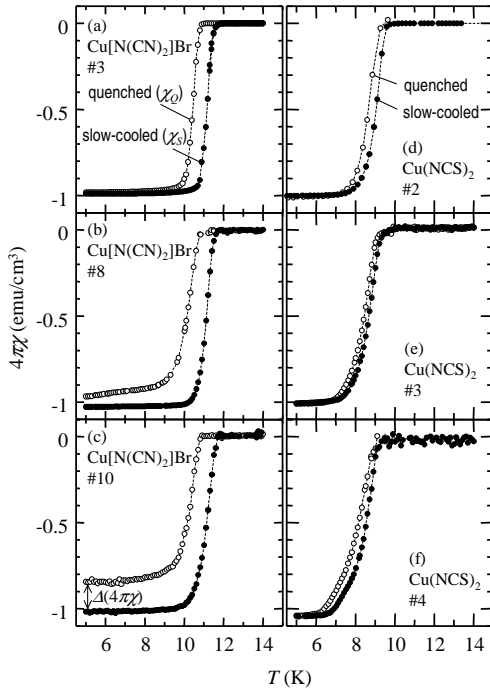


FIG. 1: Temperature dependence of the magnetic susceptibility for κ -(h8ET)₂X, where $X=\text{Cu}[\text{N}(\text{CN})_2]\text{Br}$ for panels (a)–(c) and $X=\text{Cu}(\text{NCS})_2$ for panels (d)–(f). Samples with larger index numbers have smaller crystalline sizes.^{19,22}

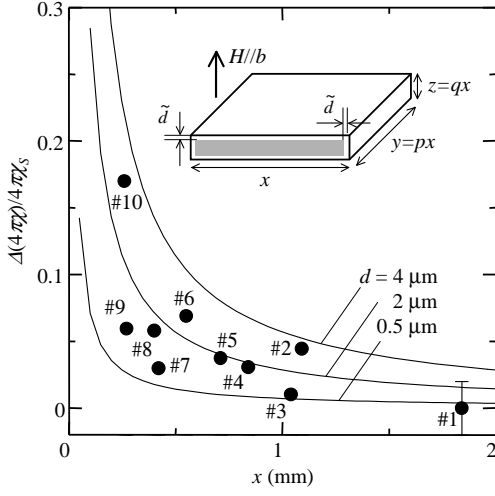


FIG. 2: Suppression of superconducting volume fraction by quenching in κ -(h8ET)₂Cu[N(CN)₂]Br. The inset shows a schematic view of the sample dimensions. Based on a rectangular shell-type insulating model, the solid curves are obtained from Eq. 1 for shell thicknesses of $\tilde{d} = 0.5, 2$, and $4 \mu\text{m}$.

In the present report, we suggest that the SC state in κ -(h8ET)₂Cu[N(CN)₂]Br (abbreviated as κ -h8ET-Br, where h8ET is conventional hydrogenated BEDT-TTF) after fast cooling coexists with non-SC (insulating) portions in the micrometer scale in the vicinity of the crystalline surface. We prove this by two experiments. In the first experiment, a marked size effect on the SC volume fraction is obtained from static magnetic susceptibility measurements. On the basis of a crude model, we propose that the mean depth of the insulating region is a few μm from the surface. In the second experiment we directly image an insulating region of 50–100 μm diameter by scanning microregion infrared reflectance spectroscopy (SMIS) measurements.^{17,18} This technique is insensitive to the surface condition of the first several layers and thus is suitable for the present study. The very large reported $\lambda_{\parallel}(0)$ (~ 24 –100 μm) can be reasonably well explained by the existence of thin insulating domains in the surface vicinity.

II. EXPERIMENTS

Single crystals of κ -h8ET-Br were grown by a standard electrochemical oxidation technique. The crystalline shape of κ -h8ET-Br is typically rectangular with (010) rhombus facets (inset of Fig. 2).

Static magnetic susceptibility measurements were performed using a SQUID magnetometer (Quantum Design, MPMS-5XL). To investigate the crystalline size effect, we chose 10 single crystals (#1 to #10).¹⁹ The samples with larger index numbers have smaller crystalline size. A magnetic field of 3 Oe was applied perpendicular to the conduction plane. The susceptibilities were

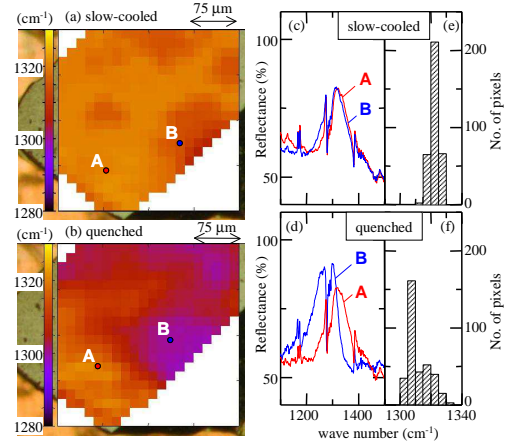


FIG. 3: (color online) (a)¹⁸, (b) Peak frequency maps of the $\nu_3(a_g)$ mode of κ -(h8ET)₂Cu[N(CN)₂]Br at 4 K. (c), (d) Reflectance spectra at A- and B-sites in Figs. 2 (a) and (b), respectively. (e), (f) Histograms of the $\nu_3(a_g)$ peak frequency.

measured in a zero-field cooling condition, giving shielding curves. A very fast cooling procedure (~ 100 K/min) from room temperature to 15 K was first adopted, giving the “quenched” (Q) state. Then a second cooling process was carried out with 0.2 K/min after warming to 100 K, giving the “slow-cooled” (S) state. The demagnetization factor was corrected using an ellipsoidal approximation.

SMIS studies were performed using a synchrotron radiation beam at the BL43IR in SPring-8.²⁰ Polarized reflectance spectra were measured on the conductive *ca*-plane with the electric field parallel to the *a*-axis by use of a Fourier transform infrared (FTIR) spectrophotometer from 500 to 2500 cm^{-1} . A single crystal of κ -h8ET-Br with dimensions approximately $0.5 \times 0.3 \times 0.1 \text{ mm}^3$ (the same sample as used in Ref. 18) was attached to a thermal anchor with carbon paste. The sample was cooled slowly at a rate of ~ 0.4 K/min from room temperature to 4 K, giving the S state. After the SMIS measurement in the S state, the temperature was increased to 120 K and then cooled at a rate of ~ 35 K/min, giving the Q state.

III. RESULTS

Figures 1(a)–1(c) show the temperature dependences of the magnetic susceptibility in κ -h8ET-Br for single crystals with different sample sizes. Regardless of sample size, an almost perfect Meissner effect is realized in the S state (filled circles). In the large sample #3, shown in Fig. 1(a), there is no change in the SC volume between the S and Q states within the experimental error. This is consistent with previous reports.^{15,21} In contrast, suppression of the SC volume in the Q state can be seen with decreasing sample size (for samples #8 and #10 in Figs. 1(b) and 1(c), respectively). The difference in the SC volume between the two cooling condi-

tions, $\Delta(4\pi\chi) = 4\pi\chi_Q - 4\pi\chi_S$, is pronounced in the smaller crystals, where $4\pi\chi_Q$ and $4\pi\chi_S$ are for the Q and S states at 5 K, respectively. In Fig. 2, the values of $\Delta(4\pi\chi)/4\pi\chi_S$ in κ -h8ET-Br are plotted as a function of x , representing the fraction of the non-SC portion, where x is the longest length of the crystal (see inset in Fig. 2). In spite of large scatter in the data, $\Delta(4\pi\chi)/4\pi\chi_S$ increases with decreasing x . The data scattering is due mainly to the sample dependence of the distribution and morphology in the insulating regions.

To confirm whether this anomalous phenomenon is characteristic of κ -h8ET-Br, similar measurements were performed for four samples of κ -(h8ET)₂Cu[N(CN)₂]₂.²² The magnetic susceptibilities are shown in Figs. 1(d)–1(f). Although T_c in the Q state is slightly lower by about 0.2–0.3 K than in the S state, an almost perfect Meissner effect is obtained for both the cooling states, independent of sample size. We therefore conclude that the effect of crystalline size on SC suppression is a peculiar feature in quenched κ -h8ET-Br. As directly indicated below, the non-SC region in the Q state is interpreted as a coexisting insulating phase in the surface vicinity.

In SMIS measurements, a shift of the fully symmetric molecular vibration mode $\nu_3(a_g)$ can be a relevant indicator of the electronic state, because it is very sensitive to the difference between the SC (metallic) and insulating phases.²³ Peak frequency maps of the ν_3 mode are shown in Figs. 3(a)¹⁸ and 3(b) for the S and Q states, respectively. In these maps brighter colors represent higher frequencies. In the S state, the peak frequency shows good spatial homogeneity at approximately 1320 cm⁻¹. The SC phase gives a higher frequency in the ν_3 mode at low temperatures,²³ demonstrating that the homogeneous SC state appears in the S state. On the other hand, in the map of the Q state (Fig. 3(b)), we find dark areas with much lower frequency than for the SC phase. As shown in Fig. 3(d), the peak of the ν_3 mode in the dark area (B-site) is shifted toward lower frequency compared with that in the remaining bright area (A-site). The corresponding reflectance spectra at almost the same positions in the S state are very similar (Fig. 3(c)). Thus, the inhomogeneous frequency map in the Q state clearly indicates the coexistence of SC and insulating regions. Figures 3(e) and 3(f) show peak frequency histograms. The histogram in the S state has a narrow maximum at 1320–1330 cm⁻¹, whereas that in the Q state is spread over 1300–1330 cm⁻¹ with a double peak structure, reflecting spatial inhomogeneity in the Q state.

IV. DISCUSSION

In the phase diagram of the κ -(ET)₂ X system,²⁴ the SC and antiferromagnetic Mott insulating (AFI) phases appear next to one another. The ground state in κ -h8ET-Br is the SC phase, while the fully deuterated salt κ -(d8ET)₂Cu[N(CN)₂]₂Br (abbreviated as κ -d8ET-Br, where d8ET is fully-deuterated BEDT-TTF), has an

AFI ground state accompanied by a minor SC phase (phase separation).^{25,26} Deuteration therefore changes the ground state from the SC to AFI phase through a first-order Mott transition.^{21,27} This is likely caused by a structural modulation in the slight change of the bond length between C-H and C-D bonds, i.e., chemical pressure. The decrease of the bandwidth W by deuteration results in an increase in U/W , where U is the on-site Coulomb interaction. This leads to a crossing of the Mott boundary toward the AFI ground state.

The minor SC phase in κ -d8ET-Br is further suppressed by faster cooling, though it was believed that superconductivity in κ -h8ET-Br is robust even after fast cooling.^{15,21,27,28,29,30} Furthermore, in ¹³C-NMR studies of κ -h8ET-Br after fast cooling, no trace of the AFI phase has been observed.³¹ On the contrary, a marked crystalline size effect on the SC volume fraction in the Q state is found, reflecting macroscopic suppression of superconductivity and an insulating region with 50–100 μ m diameter is directly observed by the SMIS technique.

Recently, macroscopic phase separation has been found near the Mott transition for the d8ET molecular substituted system κ -[(h8ET)_{1-x}(d8ET)_x]₂Cu[N(CN)₂]₂Br by the same SMIS measurement.^{17,18} For the Q state with $x = 0.7$, it was observed that the dominant insulating region contains a small SC region.¹⁸ This corresponding to a SC volume fraction suppressed to much less than $\sim 10\%$.¹⁸ Similarly, the present insulating region observed in quenched κ -h8ET-Br (an end-member with $x = 0$) seems to grow over a wide area of 50–100 μ m diameter. At first sight, one might regard the result for $x = 0$ as evidence that large portions of the sample volume become insulating. This is however inconsistent with the large SC volume even in the Q state of 80–90% (Fig. 1(c)). We here note that the skin depth δ in the SMIS measurement, $\delta = c/(2\pi\omega\sigma)^{1/2}$, is roughly estimated to be 0.7 μ m, where c is the speed of light and using the values $2\pi\omega \simeq 1000$ cm⁻¹ and $\sigma \simeq 1000$ S/cm.²³ Thus, although the SMIS measurements provide satisfactory bulk properties at a depth of approximately 1 μ m, they do not give information on regions much deeper than δ from the crystalline surface. Taking account of absence of the insulating regions detectable in NMR³¹, the existence of the insulating domains at inner site will be extracted. Accordingly, we suggest that the insulating regions in quenched κ -h8ET-Br are located in the surface vicinity and the depth of the thin domain is distributed over the surface. To verify this proposal, detailed NMR measurements for a quenched single crystal with several sample sizes will be required.

In the following, we discuss the mean depth scale of the thin domain. A crude model can explain the SC suppression in the Q state, suggesting that the insulating region extends down to a depth of ~ 2 μ m.

For the magnetic susceptibility measurements, we chose samples with a similar dimensional ratio of $x/x:y/x:z/x \simeq 1:0.9:0.2$. We here adopt the longest length x as the parameter representing the sample size,

namely, $y \simeq px$, $z \simeq qx$, and the sample volume $V_0 \simeq pqx^3$, where p and q are dimensionless numbers, $p = 0.9$ and $q = 0.2$. The first finding is that an almost perfect Meissner effect is observed in the S state, regardless of x . Thus the SC volume in the S state (V_S^{SC}) can be defined as the crystalline volume: $V_S^{SC} \simeq V_0$. Of course the SC volume is not the same as V_0 , because the magnetic field penetrates into the surface by $\lambda_{||}$; however, it is sufficiently negligible, as shown below. The second finding is that the SC volume decreases in smaller samples by quenching, i.e., a smaller x gives a larger $\Delta(4\pi\chi)$, as shown in Fig. 2. To consider $\Delta(4\pi\chi)$ as a function of x , we here assume an SC state with a rectangular insulating shell: superconductivity in the Q state is suppressed in a mean depth \tilde{d} from all the surfaces and edges (i.e., \tilde{d} is the thickness of the thin shell shown in the inset of Fig. 2) and \tilde{d} is independent of sample size. On the basis of this assumption, the SC volume in the Q state is $V_Q^{SC} \simeq (x - 2\tilde{d})(y - 2\tilde{d})(z - 2\tilde{d})$. We finally obtain the non-SC fraction in the Q state as

$$(V_S^{SC} - V_Q^{SC})/V_S^{SC} \simeq a\tilde{d}/x \quad (1)$$

for $\tilde{d} \ll x$, where $a \equiv 2(p + q + pq)/pq = 14.2$. This fraction can be compared with the experimental values of $\Delta(4\pi\chi)/4\pi\chi_S$. In Fig. 2, $(V_S^{SC} - V_Q^{SC})/V_S^{SC}$ is depicted as a function of x for $\tilde{d} = 0.5, 2$, and $4 \mu\text{m}$ (solid curves). One can see that the curve for $\tilde{d} = 2 \mu\text{m}$ is in good accordance with the experimental data. This value of \tilde{d} is adequate for the present system, because it satisfies all the following conditions: (i) $\tilde{d} \ll x$ ($\simeq 200 \mu\text{m}$), (ii) $\tilde{d} \geq \lambda_{||}(0)$ ($\simeq 0.6\text{--}0.7 \mu\text{m}^{15}$), and (iii) $\tilde{d} \geq \delta$ ($\simeq 0.7 \mu\text{m}$). The first two conditions justify the derivation of Eq. (1) and the third guarantees that the bulk insulating properties are surely captured in the SMIS studies. Regardless of the naive assumption that the SC state is suppressed over all the surfaces, this shell-type model well explains the present crystalline size effect. Indeed, as shown in Fig. 3(b), the SC region clearly remains in the Q state. We never rule out the existence of insulating regions that penetrate further into the sample than \tilde{d} .

The existence of a macroscopic insulating phase at a depth of a few μm explains the overestimation of the fast cooling data for $\lambda_{||}(0)$ observed in the low magnetic field measurements.⁴ In the magnetization (M) measurements performed in magnetic fields higher than H_{c1} , $\lambda_{||}$ is obtained from the slope in the $M(H)$ curves, in which the influence of the insulating regions is sufficiently negligible.³² However, in the low field measurements, the correct estimation of $\lambda_{||}$ is disturbed by the shell-type insulating domain induced by fast cooling, because the magnetic field penetrates into the insulating regions. This leads to the overestimation of $\lambda_{||}(0)$ as described below. If the suppression of the SC volume is attributed to the magnetic penetration depth to the SC state from the edge, $\lambda_{||}(0)$ becomes very large, $\sim 24\text{--}100 \mu\text{m}$.⁴ However, this is an incorrect treatment because the suppressed SC volume fraction after quenching mainly contains the con-

tribution of the insulating shell with \tilde{d} , as demonstrated in Fig. 2. Accordingly, the very large $\lambda_{||}(0)$ in the low field measurements after fast cooling can be explained as being due to the influence of the shell-type insulating domain.

Finally we discuss what happens after fast cooling in κ -h8ET-Br. Two contributions originate from fast cooling. The first is the chemical pressure effect, as in the case of deuteration. As discussed in previous reports,^{21,28} fast cooling through 80 K decreases W , giving rise to an increase of U/W . Thus, the macroscopic non-SC region in quenched κ -h8ET-Br will also be a Mott insulating phase, because κ -h8ET-Br is in the vicinity of the Mott insulating phase. Indeed, no SC suppression is detected in κ -(h8ET)₂Cu(NCS)₂, which is farther from the Mott boundary. The present size effect on the SC volume and the large increase of $\lambda_{||}(0)$ observed in the low field measurements⁴ are due to the existence of the macroscopic AFI region induced by chemical pressure.

The second contribution from fast cooling is the introduction of molecular disorder. There is an internal degree of freedom in the terminal ethylene groups of the ET molecule (conformational disorder). The conformational disorder is thermally excited at room temperature³³ and is frozen into the system by fast cooling. The frozen disorder will be distributed randomly all over the sample, both in the SC and non-SC regions. The disorder in the SC region gives impurity scattering. The increase of the Dingle temperature³⁴ and the slight increase of $\lambda_{||}(0)$ observed in the high field measurements^{14,15} can be explained as the influence of quasi-particle scattering by the increase of disorder in the fast cooling process. Meanwhile, a decrease of T_c ,^{14,15,21,30} vortex pinning suppression,²⁹ and an increase of the residual resistivity³⁰ may result from both the contributions of microscopic impurity scattering and macroscopic insulating region (or boundary) formation by fast cooling.

The question as to why the insulating region grows in the vicinity of the surface is still open. A possible speculation is that much more disorders in the surface vicinity are induced by very fast cooling than those in the inner site. A very fast cooling treatment may not guarantee a homogeneous cooling state within a sample, because of a thermal flow problem. Such inhomogeneous distribution of disorders may result in the present shell type insulating state. Besides, several authors have reported unconventional electronic properties arising from the surface state.^{16,35,36} For example, in κ -(h8ET)₂Cu(NCS)₂, two kinds of photoemission spectra have been found, attributed to the different surface types.³⁵ However, the present shell-type insulating domain has a bulk scale of $\sim 2 \mu\text{m}$ in depth, which is about 700 times larger than the inter-layer distance $\sim 15 \text{ \AA}$. This seems to be too large as a coherence scale originating from the surface structure of the first layer, such as structural reconstruction. Further study will be needed to clarify this point.

V. CONCLUSION

In conclusion, we have proposed a macroscopic shell-type insulating domain in quenched κ -h8ET-Br by the observation of a marked size effect on the SC suppression and by SMIS mapping of the Q state. The thin insulating domain is located in the surface vicinity with 50–100 μm diameter and a few μm depth. The very large value of $\lambda_{\parallel}(0)$ obtained from the measurements in magnetic fields lower than H_{c1} after fast cooling can be explained well by the existence of the shell-type insulating domain.

Acknowledgments

The authors thank T. Hirono, T. Kawase, and T. Moriwaki for their technical support. We are also grateful to K. Miyagawa for helpful comments. Synchrotron radiation measurements were performed at SPring-8 with the approval of JASRI (2003A0075-NS1-np and 2003B0114-NSb-np). This research was supported by a Grant-in-Aid for Scientific Research (C) from JSPS.

-
- ¹ K. Kanoda, K. Akiba, K. Suzuki, T. Takahashi, and G. Saito, Phys. Rev. Lett. **65**, 1271 (1990).
 - ² P. A. Mansky, P. M. Chaikin, and R. C. Haddon, Phys. Rev. B **50**, 15929 (1994).
 - ³ M. Pinterić, S. Tomić, M. Prester, D. J. Drobac, O. Milat, K. Maki, D. Schweitzer, I. Heinen, and W. Strunz, Phys. Rev. B **61**, 7033 (2000).
 - ⁴ M. Pinterić, S. Tomić, M. Prester, D. Drobac, and K. Maki, Phys. Rev. B **66**, 174521 (2002).
 - ⁵ D. Achkir, M. Poirier, C. Bourbonnais, G. Quirion, C. Lenoir, P. Batail, and D. Jérôme, Phys. Rev. B **47**, R11595 (1993).
 - ⁶ M. Dressel, O. Klein, G. Grüner, K. D. Carlson, H. H. Wang, and J. M. Williams, Phys. Rev. B **50**, 13603 (1994).
 - ⁷ A. Carrington, I. J. Bonalde, R. Prozorov, R. W. Gianetta, A. M. Kini, J. Schlueter, H. H. Wang, U. Geiser, and J. M. Williams, Phys. Rev. Lett. **83**, 4172 (1999).
 - ⁸ D. R. Harshman, R. N. Kleiman, R. C. Haddon, S. V. Chichester-Hicks, M. L. Kaplan, L. W. Rupp, Jr., T. Pfiz, D. Ll. Williams, and D. B. Mitzi, Phys. Rev. Lett. **64**, 1293 (1990).
 - ⁹ D. R. Harshman, A. T. Fiory, R. C. Haddon, M. L. Kaplan, T. Pfiz, E. Koster, I. Shinkoda, and D. Ll. Williams, Phys. Rev. B **49**, 12990 (1994).
 - ¹⁰ S. L. Lee, F. L. Pratt, S. J. Blundell, C. M. Aegerter, P. A. Pattenden, K. H. Chow, E. M. Forgan, T. Sasaki, W. Hayes, and H. Keller, Phys. Rev. Lett. **79**, 1563 (1997).
 - ¹¹ L. P. Le, G. M. Luke, B. J. Sternlieb, W. D. Wu, Y. J. Uemura, J. H. Brewer, T. M. Riseman, C. E. Stronach, G. Saito, H. Yamochi, H. H. Wang, A. M. Kini, K. D. Carlson, and J. M. Williams, Phys. Rev. Lett. **68**, 1923 (1992).
 - ¹² M. Lang, N. Toyota, T. Sasaki, and H. Sato, Phys. Rev. Lett. **69**, 1443 (1992).
 - ¹³ M. Lang, N. Toyota, T. Sasaki, and H. Sato, Phys. Rev. B **46**, R5822 (1992).
 - ¹⁴ A. Aburto, L. Fruchter, and C. Pasquier, Physica C **303**, 185 (1998).
 - ¹⁵ N. Yoneyama, A. Higashihara, T. Sasaki, T. Nojima, and N. Kobayashi, J. Phys. Soc. Jpn. **73**, 1290 (2004).
 - ¹⁶ M. Ishida, K. Hata, T. Mori, and H. Shigekawa, Phys. Rev. B **55**, 6773 (1997).
 - ¹⁷ T. Sasaki, N. Yoneyama, N. Kobayashi, Y. Ikemoto, and H. Kimura, Phys. Rev. Lett. **92**, 227001 (2004).
 - ¹⁸ T. Sasaki, N. Yoneyama, A. Suzuki, N. Kobayashi, Y. Ikemoto, and H. Kimura, J. Phys. Soc. Jpn. **75**, 2351 (2005).
 - ¹⁹ The sample dimensions in κ -(h8ET)₂Cu[N(CN)₂]Br for the static susceptibility measurements are as follows: $x \times y \times z$ in #1 is $1.84 \times 1.57 \times 0.34$,²⁹ #2: $1.09 \times 1.06 \times 0.13$,¹⁵ #3: $1.04 \times 0.96 \times 0.25$,²⁷ #4: $0.84 \times 0.75 \times 0.21$, #5: $0.71 \times 0.67 \times 0.17$, #6: $0.55 \times 0.47 \times 0.13$, #7: $0.42 \times 0.39 \times 0.10$, #8: $0.40 \times 0.37 \times 0.07$, #9: $0.27 \times 0.24 \times 0.04$, and #10: $0.26 \times 0.24 \times 0.07 \text{ mm}^3$.
 - ²⁰ H. Kimura, T. Moriwaki, S. Takahashi, H. Aoyagi, T. Matsushita, Y. Ishizawa, M. Masaki, S. Oishi, H. Ohkuma, T. Namba, M. Sakurai, S. Kimura, H. Okamura, H. Nakagawa, T. Takahashi, K. Fukui, K. Shinoda, Y. Kondoh, T. Sata, M. Okuno, M. Matsunami, R. Koyanagi, Y. Yoshimatsu, and T. Ishikawa, Nucl. Instrum. Methods Phys. Res. Sect. A **467-468**, 441 (2001).
 - ²¹ H. Taniguchi, A. Kawamoto, and K. Kanoda, Phys. Rev. B **59**, 8424 (1999).
 - ²² The sample dimensions in κ -(h8ET)₂Cu(NCS)₂ for the static susceptibility measurements are as follows; $x \times y \times z$ in #1 is $2.2 \times 1.1 \times 0.40$,¹⁵ #2: $2.5 \times 1.4 \times 0.26$, #3: $0.72 \times 0.41 \times 0.08$, and #4: $0.32 \times 0.20 \times 0.07 \text{ mm}^3$.
 - ²³ T. Sasaki, I. Ito, N. Yoneyama, N. Kobayashi, N. Hanasaki, H. Tajima, T. Ito, and Y. Iwasa, Phys. Rev. B **69**, 064508 (2004).
 - ²⁴ K. Kanoda, Hyperfine Interact. **104**, 235 (1997).
 - ²⁵ A. Kawamoto, K. Miyagawa, and K. Kanoda, Phys. Rev. B **55**, 14140 (1997).
 - ²⁶ K. Miyagawa, A. Kawamoto, and K. Kanoda, Phys. Rev. Lett. **89**, 017003 (2002).
 - ²⁷ N. Yoneyama, T. Sasaki, and N. Kobayashi, J. Phys. Soc. Jpn. **73**, 1434 (2004).
 - ²⁸ H. Taniguchi, K. Kanoda, and A. Kawamoto, Phys. Rev. B **67**, 014510 (2003).
 - ²⁹ N. Yoneyama, T. Sasaki, T. Nishizaki, and N. Kobayashi, J. Phys. Soc. Jpn. **73**, 184 (2004).
 - ³⁰ X. Su, F. Zuo, J. A. Schlueter, M. E. Kelly, and J. M. Williams, Phys. Rev. B **57**, R14056 (1998).
 - ³¹ K. Miyagawa (private communication).
 - ³² Provided all the crystalline volume of κ -(h8ET)₂Cu[N(CN)₂]Br in the sample of Ref. 15 become the AFI state, the maximum value of M is approximately $2 \times 10^{-3} \text{ emu}$, with assuming $S=1/2$ per ET dimer. This is two orders of magnitude lower than the reversible SC magnetization, $M \geq 0.1 \text{ emu}$ (see Fig. 6 in Ref. 15), indicating the negligible contribution of the insulating thin domain to the magnetization measurements in the mixed state.
 - ³³ H. Urayama, H. Yamochi, G. Saito, S. Sato, A. Kawamoto, J. Tanaka, T. Mori, Y. Maruyama, H. Inokuchi, Chem. Lett. **1988**, 463 (1988).

- ³⁴ T. F. Stalcup, J. S. Brooks, and R. C. Haddon, Phys. Rev. B **60**, 9309 (1999).
- ³⁵ J. E. Downes, K. E. Smith, A. Y. Matsuura, I. Lindau, and J. A. Schlueter, Surf. Sci. **551**, 219 (2004).
- ³⁶ M. Sing, U. Schwingenschlögl, R. Claessen, M. Dressel, and C. S. Jacobsen, Phys. Rev. B **67**, 125402 (2003).